Available online at website: https://journal.bcrec.id/index.php/bcrec

Bulletin of Chemical Reaction Engineering & Catalysis, 20 (4) 2025, 672-682

Original Research Article

Ultrasonic-Assisted Transesterification of Tripalmitin Using Limestone-Derived CaO Catalyst

Rakhma Amalia Nurdina[1], Yuichi Kamiya[2], Adhi Dwi Hatmanto[1], Fajar Inggit Pambudi[1], S. Suyanta[1], N. Nuryono[1]*

[1]Department of Chemistry, Faculty of Mathematics and Natural Sciences, Universitas Gadjah Mada, Sekip Utara, Yogyakarta 55281, Indonesia.
[2]Faculty of Environmental Earth Science, Hokkaido University, Nishi 5, Kita 10, Kita-ku, Sapporo 060-0810, Japan.

Received: 29th July 2025; Revised: 22th September 2025; Accepted: 23th September 2025
Available online: 1st October 2025; Published regularly: December 2025

Abstract

In producing palm oil-based biodiesel (fatty acid methyl esters) through the transesterification of triglycerides with methanol, a high-performance and straightforward catalyst is required. This research studies the synthesis and characterization of limestone-derived calcium oxide as a heterogeneous base catalyst for the transesterification of tripalmitin, a representation of palm oil triglycerides, with methanol to produce methyl palmitate. Limestone was calcined at 800 °C to produce CaO. The resulting catalyst was characterized using TGA, XRD, FTIR, SAA, and CO_2-TPD. The catalytic performance was compared with that of commercial calcium oxide under optimal reaction conditions, namely 50 °C temperature, 60 min reaction time, and 30 mg catalyst mass. The results showed that limestone-derived CaO produced a higher yield (44.6%) than commercial CaO (32.3%). The kinetics study showed that the reaction followed a two-order pseudo-kinetic model with a reaction rate constant value of 0.1450 L $mmol^{-1}$ min^{-1}. Overall, limestone-derived CaO proved to be an effective, inexpensive, and environmentally friendly alternative catalyst in the production of triglyceride-based biodiesel. Furthermore, the modification of CaO to enhance the catalytic activity needs to be explored further.

Keywords: Limestone; CaO; Transesterification; Tripalmitin; Methyl palmitate

How to Cite: Nurdina, R.A., Kamiya, Y., Hatmanto, A.D., Pambudi, F.I., Suyanta, S., Nuryono, N. (2025). Ultrasonic-Assisted Transesterification of Tripalmitin Using Limestone-Derived CaO Catalyst. *Bulletin of Chemical Reaction Engineering & Catalysis*, 20 (4), 672-682. (doi: 10.9767/bcrec.20456)

Permalink/DOI: https://doi.org/10.9767/bcrec.20456

1. Introduction

Global energy consumption continues to rise significantly due to population growth and increasing energy demand. Fossil fuels still account for approximately 80% of the world's total primary energy consumption, with the transportation sector utilizing around 24% [1]. The heavy reliance on fossil fuels leads to various negative impacts, such as greenhouse gas emissions [2], acid rain, global warming, ecological imbalance [3], as well as a decline in the world's fossil energy reserves [2]. Therefore, biofuels, such as biodiesel, are receiving increasing attention as environmentally friendly and sustainable alternatives.

Biodiesel is a sustainable alternative to conventional diesel because it is biodegradable, renewable, non-toxic, and environmentally friendly [4]. Additionally, biodiesel can serve as an effective solvent for combustion residues, thereby enhancing engine performance. Another advantage is its compatibility with petroleum-

* Corresponding Author.
Email: nuryono_mipa@ugm.ac.id (N. Nuryono)

based diesel, which allows blending without modifying conventional diesel engines [5].

Among the various biodiesel production methods, transesterification of oils and fats is the most commonly used method compared to other methods, such as pyrolysis, supercritical fluid extraction, microemulsion, membrane, and reactive distillation [6]. This process involves reacting triglycerides in the oil/fat with alcohol using a catalyst, resulting in fatty acid alkyl esters (FAAE) or biodiesel [7]. Although various types of alcohol can be used, methanol is the most common and is used to produce biodiesel in the form of fatty acid methyl esters (FAME). One of the biodiesel precursors is palm oil, which consists of 44% palmitic acid (saturated), 5% stearic acid (saturated), 39% oleic acid (unsaturated), and 10% linoleic acid (unsaturated) [8].

Palm oil has become the leading feedstock for biodiesel production due to its high productivity, consistent year-round availability, efficient extraction processes, and advantageous physicochemical properties [9]. Its relatively high content of long-chain hydrocarbons and a balanced ratio of saturated to unsaturated fatty acids contribute to the generation of favourable aromatic profiles in the resulting biofuel [10]. Furthermore, the moderate free fatty acid (FFA) content of palm oil (3–5%) facilitates efficient transesterification, which is essential for biodiesel synthesis. In contrast, while oils such as soybean, sunflower, and corn contain lower FFA levels (<1%) that may simplify transesterification, they typically offer lower oxidative stability and less efficient overall production. Notably, palm oil exhibits a high cetane number (60–65), exceeding that of cottonseed (50–55), sunflower (49–52), soybean (47–51), and corn oil (47–56), leading to enhanced ignition quality, more complete combustion, and reduced engine emissions [11]. These attributes render palm oil-derived biodiesel highly compatible with modern diesel engine requirements and supportive of increasingly strict environmental regulations.

Several studies have investigated the transesterification of palm oil using various catalysts and conditions to optimize biodiesel yield. For instance, the transesterification of crude palm oil catalyzed by homogeneous H_2SO_4 achieved a 90% yield at 64.5 °C over a relatively long reaction time of 150 minutes [12]. In contrast, Gu *et al.* employed KOH along with mixed dimethyl/diethyl carbonate as alcohol donors, achieving a 90.8% yield at a higher temperature of 100 °C and an extended reaction time of 20 hours [13].

A significant improvement in reaction efficiency was reported with heterogeneous catalysts. De & Boxi (2020) used a Cu/TiO_2 catalyst and achieved a 90.93% yield at a milder temperature of 45 °C within just 45 minutes, using a relatively high methanol-to-oil molar ratio of 20:1 [14]. Zhang *et al.* further demonstrated the efficacy of zeolite as a solid base catalyst, obtaining an impressive 99.68% yield at 65 °C within 47 minutes using a 12:1 molar ratio [15]. Moreover, Ajala *et al.* utilized catalyst derived from waste chicken eggshells for palm kernel oil transesterification, achieving a 97.1% yield at 50 °C with only 1 hour of reaction time and a 10:1 methanol-to-oil ratio [16]. Heterogeneous catalysts, particularly those derived from low-cost or waste materials, show strong potential for scalable and sustainable biodiesel production from palm oil feedstocks.

Catalyst performance in the transesterification reaction is crucial for improving the economic efficiency and environmental sustainability of biodiesel production. Heterogeneous base catalysts are considered safer for the environment, non-corrosive, recoverable, and reusable, and can be obtained from biological sources. They have high productivity, broad selectivity, and performance relatively unimpaired by water and free fatty acids [17]. Among various heterogeneous base catalysts, calcium oxide (CaO) is one of the most widely used because it shows high activity even under mild operating conditions. CaO is also environmentally friendly and can be synthesized from natural materials such as limestone [18], eggshells [18], snail shells [19], marble dust waste [20], and animal bones [21].

Based on this background, this study aims to synthesize CaO from limestone via calcination and compare its characteristics and performance with commercial CaO in tripalmitin transesterification. Tripalmitin, a triglyceride of palmitic acid, was chosen in this research as sample representation due to the high content of this triglyceride in palm oil (44%) [8]. Several previous studies of tripalmitin transesterification have been reported [22-24]. In this reported research, the reaction process was conducted using ultrasonication to evaluate the potential synergy between natural source-based heterogeneous catalysts and non-conventional energy activation techniques. The evaluation was conducted through physical and chemical characterization of the catalysts and catalytic performance testing based on the yield of the reaction products.

Although CaO-catalyzed transesterification and ultrasound-assisted biodiesel production have been extensively studied, most works focus on vegetable oils, such as: palm [16], used cooking oil [18,20], and Hydnocarpus wightiana oil [19]. Limited studies have used pure triglycerides, such as tripalmitin, as model compounds to provide a clearer understanding of reaction kinetics and mechanisms. Furthermore, the direct comparison between limestone-derived CaO and commercial

CaO as catalysts in ultrasonic-assisted systems has not been comprehensively reported. In this work, we emphasize the effect of catalyst origin and physicochemical properties on transesterification activity. The combination of detailed catalyst characterization and kinetic analysis provides insights that are important for rational catalyst design and process optimization.

2. Materials and Methods

2.1 Materials

The material used in this research was limestone taken from Ponjong, Gunung Kidul, Yogyakarta, Indonesia. Other materials were commercially available reagents, which include calcium oxide (CaO, FUJIFILM Wako), tripalmitin (Tokyo Chemical Industry Co., Ltd.), methanol CH_3OH, 99.8%, FUJIFILM Wako), and methyl palmitate (>97%, Tokyo Chemical Industry Co., Ltd.).

2.2. Preparation of Limestone-derived CaO

Ten grams of limestone powder (200 mesh) were washed with distilled water to remove surface impurities. The cleaned sample was then dried in an oven at 150 °C for 3 hours. After drying, the sample was calcinated at 800 °C for 5 hours to convert calcium carbonate ($CaCO_3$) into calcium oxide (CaO). The resulting CaO material was subsequently characterized using thermogravimetric analysis (TGA, Rigaku Thermo Plus TG 8120), X-ray fluorescence (XRF, Rigaku ZSX Primus III+), Fourier-transform infrared spectroscopy (FTIR, Shimadzu Prestige 21), X-ray diffraction (XRD, Rigaku SmartLab XRD), carbon dioxide temperature-programmed desorption (CO_2-TPD, BelCAT), and surface area analysis (SAA, BELSORP-mini) with Brunauer-Emmett Teller (BET) theory.

2.3. Catalytic Performance of Limestone-derived CaO

A total of 0.0589 g (0.1 mmol) of tripalmitin and 9.6120 g (300 mmol) of methanol were placed in a closed test tube. Then, CaO catalyst was added in varying masses of 5, 10, 20, 30, 50, and 70 mg. The transesterification reaction was carried out using the ultrasonication method (frequency: 40 kHz), with temperature variations of 40 °C and 50 °C, and reaction times of 10, 20, 30, 40, 50, 60, 120, and 180 minutes. After the reaction, the catalyst was separated from the reaction mixture. A schematic diagram of the ultrasonic-assisted transesterification setup is presented in Figure 1.

Figure 1. A schematic diagram of the ultrasonic-assisted transesterification setup.

The reaction solution was then analyzed using a GC equipped with a flame ionization detector (GC-FID, GC-2025 Shimadzu, AOC-20i Autoinjector). The column used was SH-Rtx-Wax (Shimadzu). The temperature of the oven with the column started at 70 °C for 5 min, then increased to 200 °C at a rate of 10 °C/min and was maintained at 200 °C for 5 min. Pure nitrogen (N2) was used as the carrier gas, and 1 µL of liquid sample was injected into the GC. The injector and detector temperatures were set at 150 °C and 270 °C, respectively.

Quantifying methyl palmitate products was done by comparing the sample chromatogram's peak area to the methyl palmitate standard curve, so that the number of moles of methyl palmitate produced was obtained (actual mol). Furthermore, the ester yield was calculated by dividing the actual mol with the theoretical mol (the maximum amount of methyl palmitate calculated stoichiometrically), as expressed in Eq. (1).

$$Yield\ of\ Methyl\ Palmitate\ (\%) = \frac{Actual\ mol}{Theoretical\ mol} \times 100\% \quad (1)$$

2.4. Kinetic Model for the Transesterification of Tripalmitin

The transesterification of tripalmitin with MeOH is reversible, as shown in Eq. (2).

$$C_{51}H_{98}O_6 + 3CH_3OH \rightleftharpoons 3C_{17}H_{34}O_2 + C_3H_8O_3 \quad (2)$$

Tripalmitin + 3 MeOH ⇌ 3 Methyl Palmitate + Glycerol

Because of the large excess of methanol in the reaction, the concentration in the reaction is considered constant. Furthermore, the kinetics of the transesterification reaction were tested with pseudo-zeroth-order Eq. (3), pseudo-first-order Eq. (4), and pseudo-second-order Eq. (5) kinetic models.

$$Y = \frac{kt}{C_0} \quad (3)$$

$$-ln\,(1-Y) = kt \quad (4)$$

$$\frac{1}{(1-Y)} = 1 + kC_0t \quad (5)$$

The reaction order was determined by fitting the experimental data using the reaction equations, where Y is the yield of methyl palmitate.

3. Results and Discussion

3.1. Characterization of the Catalyst

The results of X-ray fluorescence (XRF) analysis (Table 1) of the limestone samples show that the main component of this material, presented in oxides, is calcium oxide (CaO) with a mass percentage of 90.70% in oxide equivalent. At the same time, the XRD pattern confirms that the main crystalline phase is calcite ($CaCO_3$). This indicates that the limestone used is a high-quality limestone with a very dominant calcite ($CaCO_3$) content [25]. In addition to CaO component, the limestone also contains small amounts of inorganic impurities, including Al_2O_3 (4.81%), SiO_2 (3.71%), and P_2O_5 (0.45%). The high CaO content is essential in various applications, especially as a precursor in the synthesis of base catalysts such as active CaO for transesterification [26].

Thermogravimetric analysis (TGA) was performed in a nitrogen (N_2) atmosphere to observe the thermal decomposition behavior of natural limestone and determine the appropriate calcination temperature to obtain calcium oxide (CaO). Based on Figure 2a, the TGA curve of the limestone sample (black line) exhibits a single stage of significant mass loss, starting at ~650 °C and ending at around 800 °C, with a total mass loss of 47%. This mass loss is related to the decomposition of calcium carbonate ($CaCO_3$) into calcium oxide (CaO) and carbon dioxide gas (CO_2), according to Eq. (6).

$$CaCO_{3(s)} \rightarrow CaO_{(s)} + CO_{2(g)} \quad (6)$$

Based on these profiles, it can be concluded that the decarbonization process is effective starting at 650 °C and finishing at around 800 °C. Therefore, the optimal calcination temperature for full conversion to CaO in this study was 800 °C. This result aligns with previous reports that $CaCO_3$ decomposition occurs in a 650-900 °C temperature range, depending on particle size, purity, and atmospheric conditions during heating [27]. In contrast, the TGA curve of calcined limestone CaO (red line) shows a mass decrease of ~3.2% throughout the heating to 1000 °C. This indicates that the resulting CaO material is thermally stable, does not undergo further decomposition, and contains no significant amounts of residual carbonate compounds [28].

The FTIR spectra of limestone and limestone-derived CaO are shown in Figure 2b. In the spectra of limestone, typical carbonate absorption bands are clearly visible, as shown in the bands at 1427 cm^{-1}, 879 cm^{-1}, and 712 cm^{-1} [29]. The presence of these bands indicates that the primary material in limestone is calcium carbonate ($CaCO_3$). In addition, the absorption band in the 439 cm^{-1} region can be attributed to the Ca-O bond in the $CaCO_3$ structure [30]. After calcination, the spectra of limestone-derived CaO show significant changes. The intensity of the carbonate bands decreased sharply, indicating that the carbonate groups had been thermally decomposed. Although

Table 1. Chemical composition of limestone.

Component	Percentage of mass (%)
CaO	90.70
Al_2O_3	4.81
SiO_2	3.71
P_2O_5	0.45
Fe_3O_4	0.23
TiO_2	0.06
K_2O	0.02
Other	0.02

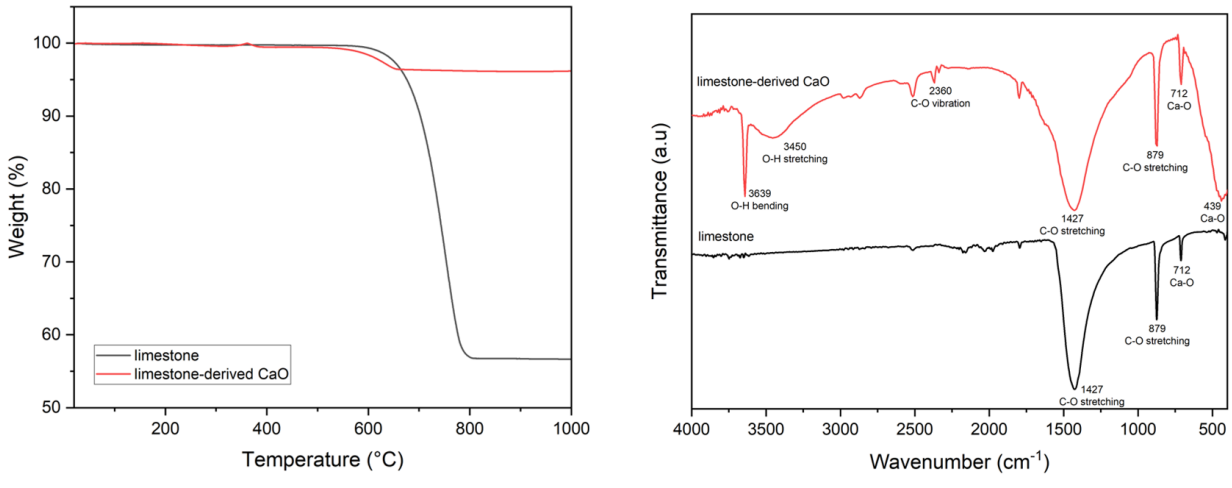

(a) (b)

Figure 2. (a) TG profiles and (b) FTIR spectra of limestone and limestone-derived CaO.

the bands at 1427 cm^{-1} and 879 cm^{-1} are still detected, their intensity is much lower than that of limestone. In addition, new bands at 3450 cm^{-1} and 3639 cm^{-1} appear, corresponding to the O-H stretching and bending vibrations of water or hydroxyl groups adsorbed on the CaO surface, respectively [31]. This suggests that CaO has an affinity for moisture and can partially form $Ca(OH)_2$ when exposed to air [31]. The band at 2360 cm^{-1} suggests the possibility of physically adsorbed CO_2 vibrations on the surface, a common phenomenon in basic materials such as CaO [32]. Meanwhile, the band at 439 cm^{-1} still appears and can be attributed to metal-oxygen (Ca-O) vibrations in the crystalline structure of CaO [29].

Figure 3 shows the X-ray diffraction (XRD) patterns of three different materials, namely limestone, limestone-derived CaO, and commercial CaO. The XRD diffraction pattern of limestone exhibits intense peaks that match the calcite ($CaCO_3$) phase, as indicated by JCPDS No. 05-0586 [33]. The dominant peaks are located at $2\theta \approx 29.4^\circ$, 36.0° , 39.4° , 43.1° , and 48.5° , which are the (104), (110), (113), (202), and (018) planes of calcite crystals [34]. After calcination, the samples showed significant changes in the XRD patterns. In the calcined CaO, peaks associated with calcite were no longer detected. Instead, new peaks appeared at $2\theta \approx 32.2^\circ$, 37.3° , and 53.8° , which correspond to the (111), (200), and (220) planes of calcium oxide (CaO) crystals [35], based on JCPDS No. 37-1497 [36]. In commercial CaO, the diffraction pattern exhibits a high degree of similarity with that of CaO from calcined limestone. This confirms that CaO obtained from limestone through calcination has a crystalline quality equivalent to that of commercial products, making it a promising catalyst alternative for application in transesterification reactions.

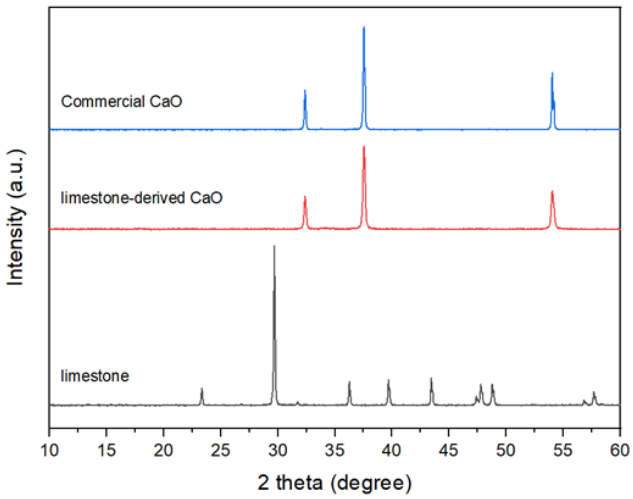

Figure 3. XRD patterns of limestone, limestone-derived CaO, and commercial CaO.

XRD analysis of crystallinity revealed that limestone exhibited a crystallinity of 81.87%, while limestone-derived CaO reached 85.98%, and commercial CaO showed 86.24%. The crystallinity of limestone-derived CaO was very close to that of commercial CaO, suggesting that natural limestone can produce catalysts with structural quality comparable to synthetic ones. This finding highlights the potential of limestone as an economical and environmentally friendly precursor for CaO-based catalysts in transesterification reactions.

The nitrogen adsorption-desorption isotherms are shown in Figure 4, and physical parameters such as specific surface area, total pore volume, and pore diameter of commercial CaO and limestone-derived CaO were calculated and are summarized in Table 2. Commercial CaO (Figure 4a) exhibited isotherm type IV according to the IUPAC classification, which is characterized by increased adsorption at relatively high pressures ($P/P_0 > 0.8$) and the formation of a small hysteresis loop between the adsorption and desorption curves. The BET-specific surface area of commercial CaO was measured at 3.87 m^2/g, a typical value for CaO with an open morphology and light mesoporous pore structure. In contrast, CaO obtained from limestone calcination showed an isotherm closer to type III, with a slight increase in adsorption volume at P/P_0 close to 1, with no apparent hysteresis loop (Figure 4b). This suggests that the material has weak interactions between the solid surface and N_2 molecules and is likely to be nonporous or contain large macropores due to particle agglomeration during calcination. This is also reflected in the very low specific surface area of only 0.12 m^2/g. The low BET surface area of limestone-derived CaO is likely due to thermal sintering and crystallite growth that occur during the calcination process at high temperatures, resulting in pore loss and decreased surface accessibility [37].

Table 2. The physical properties of CaO catalysts.

Catalyst	Surface area (m^2/g)	Total pore volume (cm^3/g)	Average pore diameter (nm)
Commercial CaO	3.87	0.02	19.71
Limestone-derived CaO	0.12	6.86	1.33

Even showing the lower surface area, limestone-derived CaO shows higher total pore volume compared to commercial CaO. This contradiction can be explained using the difference in pore structure: the limestone-derived CaO is dominated by a high number of small pores, which collectively contribute to larger total pore volume but do not provide extensive accessible surface area for N_2 adsorption. Conversely, the larger mesopores in commercial CaO facilitate a greater accessible surface area, although the overall pore volume remains relatively low due to the smaller number of pores. This relationship demonstrates that surface area, pore volume, and pore diameter are interdependent. A high pore volume does not necessarily correspond to a high surface area, as the accessibility and distribution of pores strongly influence BET results [38].

These results agree with the characterization of CO_2-TPD (Figure 4c), which shows one major desorption peak at around 640 °C, with a total basicity value of 3.07×10^{-5} mol/g. The desorption peak at high temperatures indicates the dominance of strong base sites, which are usually associated with O^{2-} ions from the crystalline CaO surface [39]. However, the relatively low value of total basicity indicates the limited number of total base sites available. This low basicity can be attributed to the low specific surface area and limited porosity, which reduces the number of active sites that interact with CO_2 molecules. In addition, thermal sintering during the limestone calcination process likely causes particle agglomeration and crystallite growth, which results in reduced exposure to the active surface [27]. This is an essential concern in designing CaO-based catalytic materials, where surface area enhancement and morphology control are key strategies to improve base site density and catalytic performance.

3.2. Catalytic Performance of Limestone-derived CaO

3.2.1 Effect of catalyst mass, temperature, and reaction time

The transesterification of tripalmitin was optimized using a limestone-derived CaO catalyst. As shown in Figure 5a, increasing the catalyst mass from 5 to 30 mg enhanced the yield from 21.7% to 44.6% due to the availability of more active basic sites. However, further increases to 50 and 70 mg led to a decline in yield, likely due to increased mixture viscosity and pore blockage, which hindered mass transfer [40]. Figure 5b shows that raising the temperature from 40 to 50 °C significantly improved the yield, driven by faster reaction rates and better methanol solubility [41]. Temperatures above this could risk methanol evaporation, thus limiting further optimization. As seen in Figure 5c, the yield increased with time, peaking at 60 minutes (44.6%), indicating reaction equilibrium. Prolonged reaction reduced yield, possibly due to methyl ester hydrolysis [41]. Therefore, the optimal transesterification conditions using a CaO catalyst were 50 °C, 30 mg of catalyst, and a 60-minute reaction time.

3.2.2 Catalytic performance of CaO for the transesterification of tripalmitin

Figure 6 shows the catalytic performance of commercial CaO and limestone-derived CaO in the transesterification reaction between tripalmitin and methanol to methyl palmitate. Limestone-derived CaO produced higher methyl ester yields (44.6%) than commercial CaO (32.3%), indicating superior catalytic activity. This difference can be explained by characterizing the physicochemical properties of both materials. The catalytic performance of limestone-derived CaO in the transesterification of tripalmitin is closely related to its physicochemical properties, as confirmed by several characterization techniques.

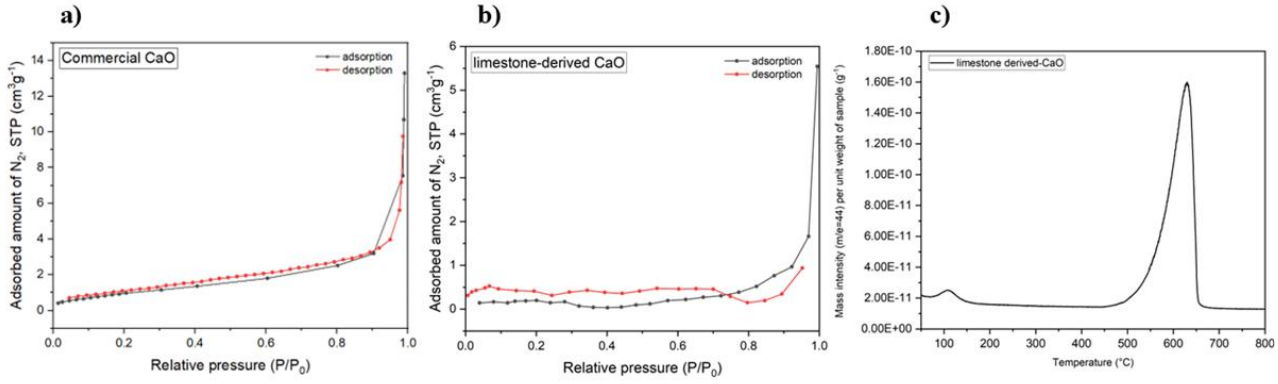

Figure 4. N_2 adsorption-desorption of (a) commercial CaO, and (b) limestone-derived CaO, and (c) CO_2-TPD profile of limestone-derived CaO.

The XRF analysis revealed that limestone is mainly composed of $CaCO_3$ with minimal impurities, ensuring that the calcination process produced CaO with high purity. This is further supported by XRD patterns, which confirmed the decomposition of $CaCO_3$ to CaO after calcination at 800 °C. The TGA analysis also verified this transformation by showing a distinct weight loss corresponding to CO_2 release, further confirming the formation of active CaO phases.

Based on BET analysis, commercial CaO has a higher specific surface area (3.87 m^2/g) compared to limestone CaO (0.12 m^2/g), which is generally associated with increased active site exposure and catalytic activity [42]. However, in this case, the better performance of limestone CaO suggests that surface area is not the main factor. Instead, the strength and number of base sites, shown through CO_2-TPD analysis, seem to have a more dominant role. Limestone CaO exhibits a high-intensity desorption peak at around 640 °C, associated with strong base sites, and has a basicity value of 3.07×10^{-5} mol/g. These strong base sites play a crucial role in the deprotonation and activation of carbonyl groups of triglyceride molecules, which are key steps in the transesterification reaction [43]. The reaction mechanism for transesterifying tripalmitin with methanol is shown in Figure 7.

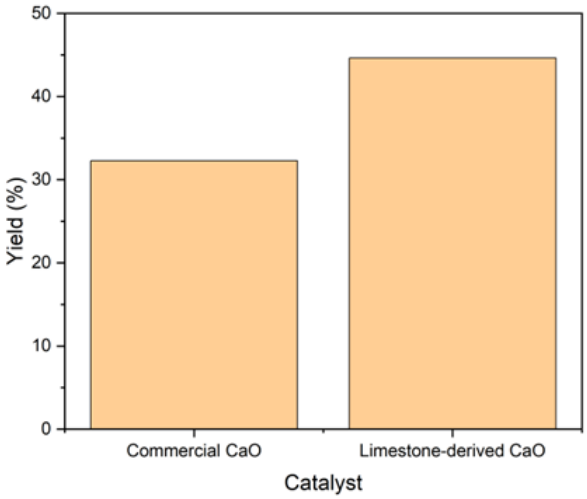

Figure 6. Catalytic performance of various catalysts for the transesterification of tripalmitin and methanol.

Table 3 presents a comparison of the performance of various heterogeneous catalysts in the transesterification of tripalmitin with methanol. From the multiple types of catalysts reviewed, the effectiveness of the catalyst is strongly influenced by the kind of material, activation method, and reaction conditions. Regarding time and temperature efficiency, the CaO from this study (both commercial and limestone-derived) showed advantages in terms of milder operating conditions. The reaction takes only 1 hour at 50 °C with ultrasonication, compared to other catalysts, such as organotin (IV), which takes 24 hours at 65 °C [22], or Mg-Al hydrotalcites, which require 120 °C for 6 hours [23].

CaO from limestone yielded 44.6%, which is higher than the commercial CaO (32.3%) despite using identical reaction conditions. This is closely related to the strong base site character of l-CaO, as indicated by CO_2-TPD data, despite its lower surface area. Meanwhile, catalysts derived from calcined shell waste [24] and hydrotalcite [23] achieve yields of nearly 90%, but require more demanding reaction conditions (high time and/or temperature) and are not economical or environmentally friendly on an industrial scale.

3.3 Kinetic Model for the Transesterification of Tripalmitin

The kinetics of tripalmitin transesterification with methanol with limestone-derived CaO catalyst at 50 °C was evaluated. By applying the zero-, one-, and two-pseudo-order kinetic models to the reaction data (Eqs. 3-5), it was found that the two-pseudo-order model was most suitable, as indicated by the highest coefficient of determination (R^2) value (Figure 8). The value of

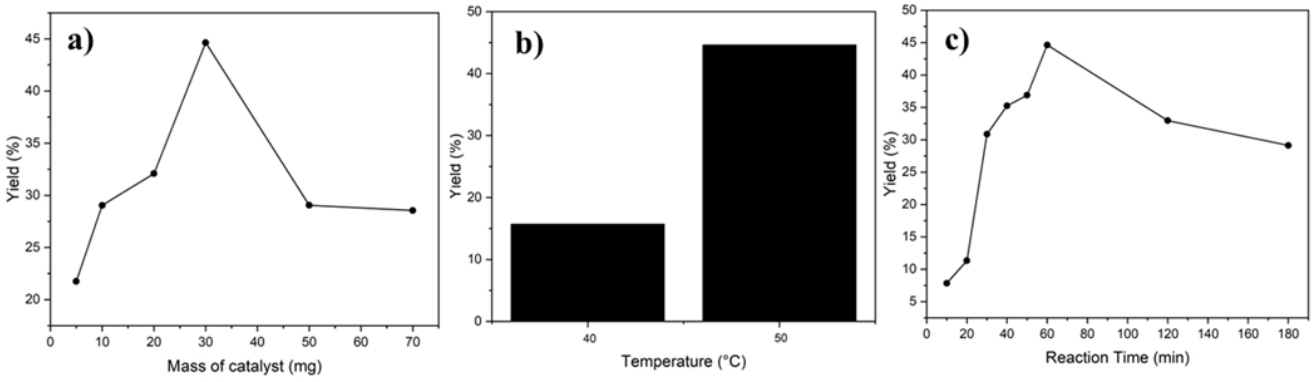

Figure 5. Optimization parameters of (a) mass of catalyst, (b) temperature, and (c) time for the transesterification of tripalmitin.

the reaction rate constant (k) obtained was 0.1450 L.mmol^{-1}.min^{-1}. This result indicates that the reaction rate depends on the concentration of reactants and reaction time, following the characteristics of the second-order model [45].

The use of limestone as a precursor for CaO catalyst offers qualitatively significant economic and environmental benefits. Limestone is inexpensive, abundant, and widely available, making it a cost-effective alternative to commercial CaO. The limestone-derived CaO showed a higher yield in methyl palmitate compared to commercial CaO, demonstrating its competitive catalytic capability. Furthermore, modifications such as metal doping or catalyst support can further enhance their performance and long-term stability [46].

4. Conclusions

CaO synthesized from local limestone showed higher catalytic performance than commercial CaO in the ultrasonic-assisted transesterification reaction of tripalmitin with methanol, resulting in a methyl palmitate yield of 44.6% at optimal reaction conditions (the tripalmitin to methanol to catalyst weight ratio of 2:320:1, at 50 °C for 60 min). The high performance is supported by its basicity, which facilitates methanol activation and enhances the transesterification process. Thus, limestone-based CaO can be an effective, economical, and environmentally friendly alternative heterogeneous catalyst for triglyceride-based biodiesel production. This finding is expected to contribute to the development of economical and sustainable natural resource-based catalyst technology for biodiesel production. However, further modification of CaO is required to improve its activity.

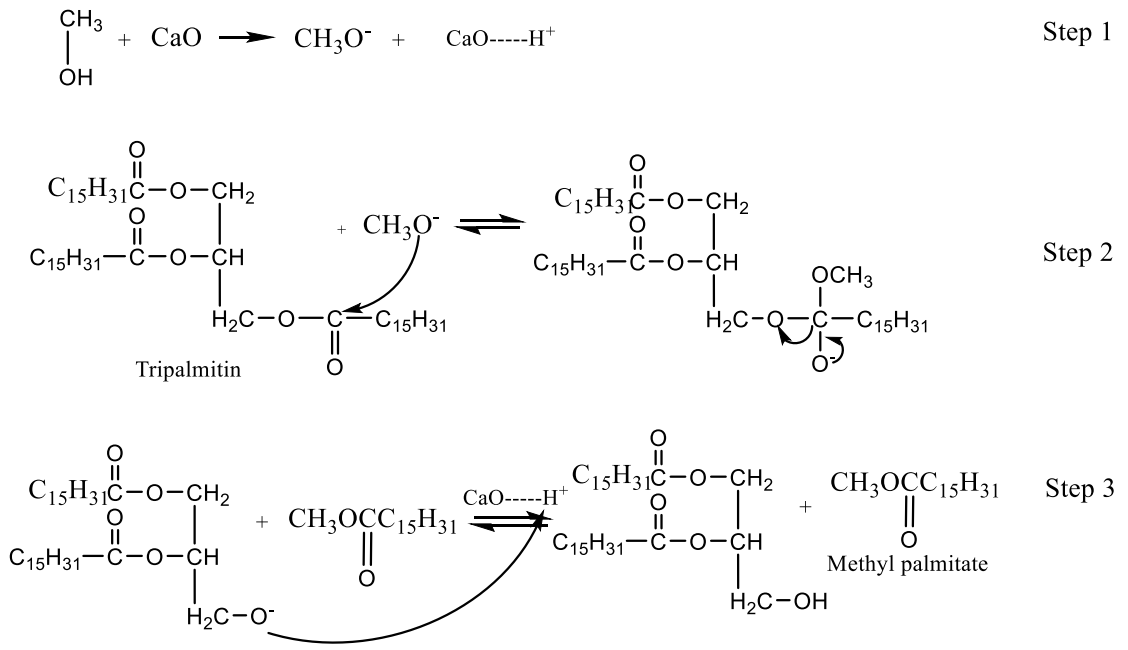

Figure 7. Reaction mechanism for the transesterification of tripalmitin with methanol.

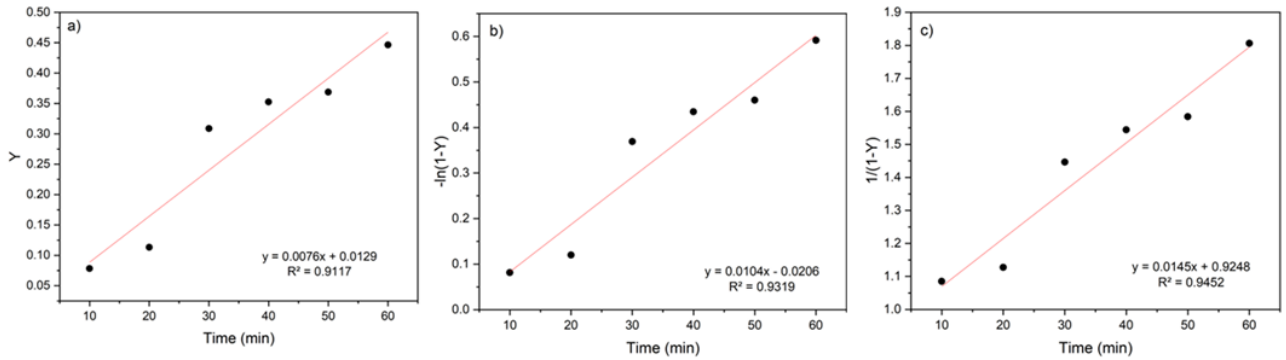

Figure 8. Transesterification kinetics plots for (a) zero, (b) first, and (c) second-order models.

Acknowledgment

The authors thank the Directorate of Research and Community Service, Directorate General of Research and Development, Ministry of Higher Education, Sciences and Technology, Republic of Indonesia, for the financial support through the Regular Fundamental Research (PFR) Scheme with the contract number: 2405/UN1/ DITLIT/Dit-Lit/PT.01.03/2025.

CRedit Author Statement

Author Contributions: R. A. Nurdina: Conceptualization, Methodology, Investigation, Resources, Data Curation, Writing, Review and Editing; Y. Kamiya: Conceptualization, Methodology, Formal Analysis, Data Curation, Writing Draft Preparation, Visualization, Software, Project Administration; A. D. Hatmanto: Investigation, Resources, Writing, Review and Editing, Validation; F. I. Pambudi: Review and Editing, Validation; Suyanta: Review and Editing, Validation; Nuryono: Conceptualization, Methodology, Investigation, Resources, Validation, Writing, Review and Editing, Data Curation. All authors have read and agreed to the published version of the manuscript.

References

[1] Amenaghawon, A.N., Amune, U.O., Ayere, J.E., Otuya, I.C., Eshiemogie, S.A., Ehiawaguan, E.I., Diemesor, G., Abuga, E.C., Oiwoh, O., Tijani, O., Oyefolu, P.K., Okoro, O.V., Shavandi, A., Anyalewechi, C.L., Elimian, E.A., Okedi, M.O., Okoduwa, I.G., Eshiemogie, S.O., Osazuwa, O., Darmokoesoemo, H., Kusuma, H.S. (2025). A comprehensive insight into the role of synthesis methods on the properties and performance of bio-derived heterogeneous catalysts for biodiesel production. *Molecular Catalysis*, 579(January), 115057. DOI: 10.1016/j.mcat.2025.115057.

[2] Peng, B., Streimikiene, D., Agnusdei, G.P., Balezentis, T. (2024). Is sustainable energy development ensured in the EU agriculture? Structural shifts and the energy-related greenhouse gas emission intensity. *Journal of Cleaner Production*, 445(November 2023), 141325. DOI: 10.1016/j.jclepro.2024.141325.

[3] Zhou, X., Patel, G., Mahalik, M.K., Gozgor, G. (2024). Effects of green energy and productivity on environmental sustainability in BRICS economies: The role of natural resources rents. *Resources Policy*, 92(March), 105026. DOI: 10.1016/j.resourpol.2024.105026.

[4] Okoro, O.V., Preat, V., Karimi, K., Nie, L., Debaste, F., Shavandi, A. (2023). Optimizing the subcritical water valorization of insect (Hermetia illucens l.) farming waste for biodiesel production. *Chemical Engineering Research and Design*, 196, 413–426. DOI: 10.1016/j.cherd.2023.06.043.

[5] Rozina, Ahmad, M., Zafar, M. (2023). Synthesis of green and non-toxic biodiesel from non-edible seed oil of Cichorium intybus using recyclable nanoparticles of MgO. *Materials Today Communications*, 35(February), 105611. DOI: 10.1016/j.mtcomm.2023.105611.

[6] Ghosh, N., Patra, M., Halder, G. (2024). Current advances and future outlook of heterogeneous catalytic transesterification towards biodiesel production from waste cooking oil. *Sustainable Energy and Fuels*, 8(6), 1105–1152. DOI: 10.1039/d3se01564e.

[7] Buchori, L., Istadi, I., Purwanto, P. (2016). Advanced Chemical Reactor Technologies for Biodiesel Production from Vegetable Oils - A Review. *Bulletin of Chemical Reaction Engineering & Catalysis*, 11(3), 606-430. DOI: http://doi.org/10.9767/bcrec.11.3.490.406-430

[8] Stavila, E., Yuliati, F., Adharis, A., Laksmono, J.A., Iqbal, M. (2023). Recent advances in synthesis of polymers based on palm oil and its fatty acids. *RSC Advances*, 13(22), 14747–14775. DOI: 10.1039/d3ra01913f.

[9] Naseef, H.H., Tulaimat, R.H. (2025). Transesterification and esterification for biodiesel production: A comprehensive review of catalysts and palm oil feedstocks. *Energy Conversion and Management: X,* 26(February), 100931. DOI: 10.1016/j.ecmx.2025.100931.

[10] Istadi, I., Riyanto, T., Khofiyanida, E., Buchori, L., Anggoro, D.D., Sumantri, I., Putro, B.H.S., Firnanda, A.S. (2021). Low-oxygenated biofuels production from palm oil through hydrocracking process using the enhanced Spent RFCC catalysts. *Bioresource Technology Reports*, 14(February), 100677. DOI: 10.1016/j.biteb.2021.100677.

[11] Jayed, M.H., Masjuki, H.H., Saidur, R., Kalam, M.A., Jahirul, M.I. (2009). Environmental aspects and challenges of oilseed produced biodiesel in Southeast Asia. *Renewable and Sustainable Energy Reviews*, 13(9), 2452–2462. DOI: 10.1016/j.rser.2009.06.023.

[12] Anguebes-Franseschi, F., Córdova-Quiroz, A., Cerón-Bretón, J., Aguilar-Ucan, C., Castillo-Martínez, G., Cerón-Bretón, R., Ruíz-Marín, A., Montalvo-Romero, C. (2016). Optimization of Biodiesel Production from African Crude Palm Oil (Elaeis guineensis Jacq) with High Concentration of Free Fatty Acids by a Two-Step Transesterification Process. *Open Journal of Ecology*, 06(01), 13–21. DOI: 10.4236/oje.2016.61002.

[13] Gu, J., Gao, Y., Xu, X., Wu, J., Yu, L., Xin, Z., Sun, S. (2018). Biodiesel production from palm oil and mixed dimethyl/diethyl carbonate with controllable cold flow properties. *Fuel*, 216 (July 2017), 781–786. DOI: 10.1016/j.fuel.2017.09.081.

[14] De, A., Boxi, S.S. (2020). Application of Cu impregnated TiO2 as a heterogeneous nanocatalyst for the production of biodiesel from palm oil. *Fuel*, 265 (August 2019), 117019. DOI: 10.1016/j.fuel.2020.117019.

[15] Zhang, P., Chen, X., Leng, Y., Dong, Y., Jiang, P., Fan, M. (2020). Biodiesel production from palm oil and methanol via zeolite derived catalyst as a phase boundary catalyst: An optimization study by using response surface methodology. *Fuel*, 272 (March), 117680. DOI: 10.1016/j.fuel.2020.117680.

[16] Ajala, E.O., Ajala, M.A., Odetoye, T.E., Aderibigbe, F.A., Osanyinpeju, H.O., Ayanshola, M.A. (2021). Thermal modification of chicken eggshell as heterogeneous catalyst for palm kernel biodiesel production in an optimization process. *Biomass Conversion and Biorefinery*, 11(6), 2599–2615. DOI: 10.1007/s13399-020-00636-x.

[17] Mukhtar, A., Saqib, S., Lin, H., Hassan Shah, M.U., Ullah, S., Younas, M., Rezakazemi, M., Ibrahim, M., Mahmood, A., Asif, S., Bokhari, A. (2022). Current status and challenges in the heterogeneous catalysis for biodiesel production. *Renewable and Sustainable Energy Reviews*, 157 (December 2021), 112012. DOI: 10.1016/j.rser.2021.112012.

[18] Sisca, V., Deska, A., Syukri, Zilfa, Jamarun, N. (2021). Synthesis and characterization of CaO limestone from lintau buo supported by TiO2 as a heterogeneous catalyst in the production of biodiesel. *Indonesian Journal of Chemistry*, 21(4), 979–989. DOI: 10.22146/ijc.64675.

[19] Krishnamurthy, K.N., Sridhara, S.N., Ananda Kumar, C.S. (2020). Optimization and kinetic study of biodiesel production from Hydnocarpus wightiana oil and dairy waste scum using snail shell CaO nano catalyst. *Renewable Energy*, 146, 280–296. DOI: 10.1016/j.renene.2019.06.161.

[20] Bargole, S.S., Singh, P.K., George, S., Saharan, V.K. (2021). Valorisation of low fatty acid content waste cooking oil into biodiesel through transesterification using a basic heterogeneous calcium-based catalyst. *Biomass and Bioenergy*, 146 (September 2020), 105984. DOI: 10.1016/j.biombioe.2021.105984.

[21] Tan, Y.H., Abdullah, M.O., Kansedo, J., Mubarak, N.M., Chan, Y.S., Nolasco-Hipolito, C. (2019). Biodiesel production from used cooking oil using green solid catalyst derived from calcined fusion waste chicken and fish bones. *Renewable Energy*, 139(November 2014), 696–706. DOI: 10.1016/j.renene.2019.02.110.

[22] Yean, C.H., Das, V.G.K. (2000). Studies on the transesterification of glycerides: I. The methanolysis of tripalmitin catalysed by diorganotin(IV) compounds. *Applied Organometallic Chemistry*, 14(6), 304–315. DOI: 10.1002/(SICI)1099-0739(200006)14:6<304::AID-AOC985>3.0.CO;2-N.

[23] Liu, Y., Lotero, E., Goodwin, J.G., Mo, X. (2007). Transesterification of poultry fat with methanol using Mg-Al hydrotalcite derived catalysts. *Applied Catalysis A: General*, 331(1), 138–148. DOI: 10.1016/j.apcata.2007.07.038.

[24] Maruyama, H., Seki, H. (2022). Esterification of tripalmitin using calcined scallop shell as a heterogeneous basic catalyst. *Asia-Pacific Journal of Chemical Engineering*, 18(2). DOI: 10.1002/apj.2870.

[25] Wang, Y., He, C., Li, G., Liu, X., Liu, L., Jiao, Y. (2025). Sustainable hollow spherical CaO derived from waste eggshells for transesterification of lard: Catalytic characterization, performance and thermodynamics. *Renewable Energy*, 250 (December 2024), 123302. DOI: 10.1016/j.renene.2025.123302.

[26] Wong, Y.C., Tan, Y.P., Taufiq-Yap, Y.H., Ramli, I., Tee, H.S. (2015). Biodiesel production via transesterification of palm oil by using CaO-CeO2 mixed oxide catalysts. *Fuel*, 162, 288–293. DOI: 10.1016/j.fuel.2015.09.012.

[27] Basumatary, S.F., Brahma, S., Hoque, M., Das, B.K., Selvaraj, M., Brahma, S., Basumatary, S. (2023). Advances in CaO-based catalysts for sustainable biodiesel synthesis. *Green Energy and Resources*, 1(3), 100032. DOI: 10.1016/j.gerr.2023.100032.

[28] Pranyoto, N., Susanti, Y.D., Ondang, I.J., Angkawijaya, A.E., Soetaredjo, F.E., Santoso, S.P., Yuliana, M., Ismadji, S., Hartono, S.B. (2022). Facile Synthesis of Silane-Modified Mixed Metal Oxide as Catalyst in Transesterification Processes. *Nanomaterials*, 12(2). DOI: 10.3390/nano12020245.

[29] Jayaprabakar, J., Karthikeyan, A., Vijai Anand, K., Arunkumar, T., Anbazhaghan, N., Rangasamy, G. (2023). Synthesis and characterization of calcium oxide nano particles obtained from biowaste and its combustion characteristics in a biodiesel operated compression ignition engine. *Fuel*, 350(May), 128839. DOI: 10.1016/j.fuel.2023.128839.

[30] Gunasekaran, S., Anbalagan, G., Pandi, S. (2006). Raman and infrared spectra of carbonates of calcite structure. *Journal of Raman Spectroscopy*, 37(9), 892–899. DOI: 10.1002/jrs.1518.

[31] Amesho, K.T.T., Lin, Y.C., Chen, C.E., Cheng, P.C., Shangdiar, S. (2022). Kinetics studies of sustainable biodiesel synthesis from Jatropha curcas oil by exploiting bio-waste derived CaO-based heterogeneous catalyst via microwave heating system as a green chemistry technique. *Fuel*, 323 (February), 123876. DOI: 10.1016/j.fuel.2022.123876.

[32] Hernández-Martínez, M.A., Rodriguez, J.A., Chavez-Esquivel, G., Ángeles-Beltrán, D., Tavizón-Pozos, J.A. (2023). Canola oil transesterification for biodiesel production using potassium and strontium supported on calcium oxide catalysts synthesized from oyster shell residues. *Next Materials*, 1(4), 100033. DOI: 10.1016/j.nxmate.2023.100033.

[33] Ribeiro, P.B., de Freitas, V.O., Machry, K., Muniz, A.R.C., da Rosa, G.S. (2019). Evaluation of the potential of coal fly ash produced by gasification as hexavalent chromium adsorbent. *Environmental Science and Pollution Research*, 26(28), 28603–28613. DOI: 10.1007/s11356-018-3852-7.

[34] Render, D., Samuel, T., King, H., Vig, M., Jeelani, S., Babu, R.J., Rangari, V. (2016). Biomaterial-Derived Calcium Carbonate Nanoparticles for Enteric Drug Delivery. *Journal of Nanomaterials*, 2016. DOI: 10.1155/2016/3170248.

[35] Madhu, B.J., Bhagyalakshmi, H., Shruthi, B., Veerabhadraswamy, M. (2021). Structural, AC conductivity, dielectric and catalytic behavior of calcium oxide nanoparticles derived from waste eggshells. *SN Applied Sciences*, 3(6). DOI: 10.1007/s42452-021-04607-3.

[36] Teo, S.H., Taufiq-Yap, Y.H., Rashid, U., Islam, A. (2015). Hydrothermal effect on synthesis, characterization and catalytic properties of calcium methoxide for biodiesel production from crude Jatropha curcas. *RSC Advances*, 5(6), 4266–4276. DOI: 10.1039/c4ra11936c.

[37] Ashine, F., Kiflie, Z., Prabhu, S.V., Tizazu, B.Z., Varadharajan, V., Rajasimman, M., Joo, S.W., Vasseghian, Y., Jayakumar, M. (2023). Biodiesel production from Argemone mexicana oil using chicken eggshell derived CaO catalyst. *Fuel*, 332(P2), 126166. DOI: 10.1016/j.fuel.2022.126166.

[38] Thommes, M., Kaneko, K., Neimark, A. V., Olivier, J.P., Rodriguez-Reinoso, F., Rouquerol, J., Sing, K.S.W. (2015). Physisorption of gases, with special reference to the evaluation of surface area and pore size distribution (IUPAC Technical Report). *Pure and Applied Chemistry*, 87(9–10), 1051–1069. DOI: 10.1515/pac-2014-1117.

[39] Pudi, S.M., Biswas, P., Kumar, S. (2016). Selective hydrogenolysis of glycerol to 1,2-propanediol over highly active copper-magnesia catalysts: Reaction parameter, catalyst stability and mechanism study. *Journal of Chemical Technology and Biotechnology*, 91(7), 2063–2075. DOI: 10.1002/jctb.4802.

[40] Hájek, M., Vávra, A., Skopal, F., Straková, A., Douda, M. (2020). The description of catalyst behaviour during transesterification of rapeseed oil – Formation of micellar emulsion. *Renewable Energy*, 159, 938–943. DOI: 10.1016/j.renene.2020.06.082.

[41] Boro, J., Konwar, L.J., Deka, D. (2014). Transesterification of non edible feedstock with lithium incorporated egg shell derived CaO for biodiesel production. *Fuel Processing Technology*, 122, 72–78. DOI: 10.1016/j.fuproc.2014.01.022.

[42] Zabeti, M., Wan Daud, W.M.A., Aroua, M.K. (2009). Activity of solid catalysts for biodiesel production: A review. *Fuel Processing Technology*, 90(6), 770–777. DOI: 10.1016/j.fuproc.2009.03.010.

[43] Granados, M.L., Poves, M.D.Z., Alonso, D.M., Mariscal, R., Galisteo, F.C., Moreno-Tost, R., Santamaría, J., Fierro, J.L.G. (2007). Biodiesel from sunflower oil by using activated calcium oxide. *Applied Catalysis B: Environmental*, 73(3), 317–326. DOI: 10.1016/j.apcatb.2006.12.017.

[44] Maruyama, H., Seki, H. (2022). Esterification of tripalmitin using calcined scallop shell as a heterogeneous basic catalyst. *Asia-Pacific Journal of Chemical Engineering*, 18(2) DOI: 10.1002/apj.2870.

[45] Aniagor, C.O., Anekwe-Nwekeaku, O.J., Tabugbo, B.I. (2025). Synthesis of biodiesel from Cyperus esculentus seed oil: Investigation of temperature effect on the transesterification kinetics and bond structure. *Biomass and Bioenergy*, 197 (March), 107766. DOI: 10.1016/j.biombioe.2025.107766.

[46] Shan, R., Lu, L., Shi, Y., Yuan, H., Shi, J. (2018). Catalysts from renewable resources for biodiesel production. *Energy Conversion and Management*, 178(July), 277–289. DOI: 10.1016/j.enconman.2018.10.032.